



Original Research Article

An Optimized and Adaptive Hybrid Renewable Energy Systems Model for Enhanced Rural Electrification: A Comparative Analysis of Three Distinct Rural Areas in Namibia

Vilho. N. Nghuumbwa*¹, Tom Wanjekeche¹, Ester Hamatwi¹, Heinrich Steinhart²

¹Department of Electrical and Computer Engineering, University of Namibia, Namibia

²Department of Faculty of Electronics and Computer Science, Hochschule Aalen, Germany

e-mail: nghuumbwav@gmail.com, twanjekeche@unam.na, chamatwi@unam.na,
Heinrich.Steinhart@hs-aalen.de

Cite as: Nghuumbwa, V.N., Wanjekeche, T., Hamatwi, E., Steinhart, H., An optimized and adaptive hybrid renewable energy systems model for enhanced rural electrification: A comparative analysis of three distinct rural areas in Namibia, *J.sustain. dev. energy water environ. syst.*, 2(3), 1140703, 2026, DOI: <https://doi.org/10.13044/j.sdewes.d14.0703>

ABSTRACT

For a long period, Namibia has been facing challenges of providing electricity for its rural households despite the country's abundant renewable energy resources. The primary barrier to electrification is the remote geographical location of many rural communities. To address this issue, the study proposes an optimization model for renewable energy systems to ensure cost-effective and reliable electrification of rural areas. Non-dominated Sorting Genetic Algorithm II, a multi-objective evolutionary algorithm, is employed to determine optimal microgrid configurations that simultaneously minimize five conflicting objectives (i.e., total life cycle cost, levelized cost of electricity, loss of power supply probability, total wasted renewable energy, and carbon dioxide emissions), representing economic, technical, and environmental goals. The Hybrid Renewable Energy System considered comprises of solar, wind, biomass, and fuel cell sources, supported by battery and supercapacitor storage. The model generates a Pareto front of non-dominated solutions, illustrating trade-offs between cost, reliability, and environmental impact. Optimal solutions are then selected using a weighted sum method by applying weights of 0.35 to both the normalized levelized cost of electricity and the loss of power supply probability, 0.2 to carbon dioxide emissions, and 0.1 to total wasted power. The results are validated by case studies of 3 villages: Oluundje, Ombudiya, and Onguati, yielding a levelized cost of electricity of 0.0042 USD/kWh, 0.0023 USD/kWh, and 0.0811 USD/kWh, and reliability levels of 99.28%, 79.82% and 94.20% respectively. These results demonstrate the robustness and adaptability of the proposed optimization model and serve as valuable guidance to policymakers, investors, and international partners in enhancing rural electrification in Namibia and other regions.

KEYWORDS

Energy storage system, Hybrid renewable energy system, Renewable energy, Rural area, Optimization.

INTRODUCTION

Grid extension to remote rural areas is either not financially viable or practically infeasible, as these locations are geographically isolated and are sparsely populated, resulting in low energy demands, despite the fact that there is abundant Renewable Energy Sources (RESs) such as wind, solar, and biomass, which are a better option for electrification when the traditional grid extension is uneconomical [1]. Due to the intermittent nature of major RESs,

there is a need to embed two or more available RESs and energy storage to develop a cost-effective, reliable, and sustainable hybrid off-grid rural electrification system [2]. The study by Shaha *et al.* [3] asserted that accurate sizing of hybrid renewable energy systems (HRESs) is essential in renewable energy applications, as it ensures optimum utilization of the RESs at a minimum investment and at the desired conditions to fulfil the energy requirements of a specific load. Therefore, the development of optimization models is required to match the energy demand with the resources.

To optimize the capacity of the components in HRESs, different types of indicators (economic, environmental, reliability, and social) can be used together or separately as the objective function [4]. Electrification planning is multi-objective by nature; however, the existing rural electrification tools only consider economic objectives [5]. Currently, there is an urgent need to draw attention to achieving the Sustainable Development Goal (SDG) 7 (Affordable and Clean Energy), and other SDGs, and thus, they are to be given consideration in optimization approaches [5].

The hybrid Optimization of Multiple Energy Resources (HOMER) software has been commonly used to optimize and analyze the HRESs as well as perform sensitivity analysis for different system configurations. However, according to Zebra *et al.* [6], the HOMER model does not consider the depth of discharge of the battery, environmental impact, and cannot perform multi-objective optimization. Other computational tools, such as HYBRID 2 are used though developed based on the general idea of sizing and optimization, unfortunately, such tools require large data sets, they are less flexible, and has limited access to parameters [6]. The HYBRIDS and Transient Energy System Simulation (TRNSYS) are simulation tools that are also used for HRESs designs, but do not perform optimal sizing. The RETScreen (Clean Energy Management Software) tool is used for rough sizing, financial and emission analysis of the optimized system, as well as performance analysis, however the Solar Photovoltaic (SPV) performance does not account for the temperature effect. Subsequently, the PVsyst (Photovoltaic System) tool is developed to solely compute SPV systems or modules [7]. Therefore, to realistically model the problem, there is a need for customized multi-objective optimization approaches, considering other design variables, such as a trade-off between reliability and cost [5]. According to Dad and Saleem [8], iterative approaches, fuzzy logic-based control schemes, and analytical methods are not suitable for multi-objective optimization of hybrid renewable energy systems. Moreover, a suitable way to deal with multi-objective optimization is by using metaheuristic methods such as non-dominated sorting genetic algorithm (NSGA), and multi-objective particle swarm optimization (MOPSO), which can effectively approximate global Pareto-optimal fronts for complex, non-convex problems, though absolute global optimality is not guaranteed [9].

In [10], a comparison of NSGA-II, NSGA-III, and MOPSO for a hybrid system of SPV, wind, battery, and diesel generator was conducted with the objective of minimizing *LPSP* and *COE*. MOPSO achieved the lowest *LPSP*, while NSGA-II gave the lowest *COE*. Similarly, [11] compared MOPSO, NSGA-II, Strength Pareto Evolutionary Algorithm 2 (SPEA2), and Pareto Envelope-based Selection Algorithm 2 (PESA2) for a standard IEEE 30-bus six-generator system, considering power flow and system constraints. MOPSO outperformed other methods in minimizing generation cost and emissions, but its complexity due to genetic operator handling was noted. In [12], NSGA-II and MOPSO were applied to a solar-wind-battery system, aiming to minimize *LPSP* and *COE*. NSGA-II proved to be more accurate, while MOPSO was faster and achieved a lower *LPSP*. The difference between the two methods was marginal, suggesting that both are viable. Lastly, [13] applied NSGA-II and MOPSO to a more complex system including solar, wind, electrolyser, hydrogen storage, PEMFC, and thermal storage, targeting energy savings and grid integration. Both methods showed similar performances in meeting objective functions, indicating their robustness in multi-source energy systems. Maheri [9] emphasized the growing importance of metaheuristic algorithms such as NSGA-II and MOPSO for multi-objective hybrid renewable energy system

optimization, noting their ability to approximate global Pareto-optimal fronts more effectively than traditional deterministic algorithms like ϵ -constraint and weighted-sum methods. Building on this foundation, Vijai and Bagavathi [14] demonstrated that NSGA-II's non-dominated sorting and crowding-distance mechanisms preserve population diversity and ensure rapid convergence toward the true Pareto front. Furthermore, Pinto-Roa *et al.* [15] highlighted the evolutionary nature of NSGA-II, whose genetic operators (selection, crossover, and mutation) enable robust global search, minimize the risk of local entrapment, and maintain computational scalability in nonlinear and discrete optimization environments. These characteristics make NSGA-II particularly suitable for renewable energy system optimization, where design variables are often nonlinear, discontinuous, and conflicting, for instance, balancing economic cost, reliability, and environmental impact in multi-source systems involving solar, wind, biomass, and energy storage. Its ability to generate diverse Pareto-optimal solutions allows decision-makers to evaluate trade-offs and select the most technically and economically feasible HRES configurations. Considering that the NSGA-II provides a Pareto front of optimal solutions with high accuracy and low cost of energy, a modified NSGA-II called a weighted NSGA-II was developed in this study to handle five simultaneous objectives: total life cycle cost (*TLCC*), levelized cost of electricity (*LCOE*), loss of power supply probability (*LPSP*), total wasted renewable energy (*WRE*), and carbon dioxide (CO_2) emissions, ensuring balanced trade-offs between cost, reliability, and environmental impact as detailed in Section III. The NSGA-II algorithm is provided in [Figure 1](#).

Load profile estimation remains one of the most significant challenges in non-electrified rural areas, particularly in Sub-Saharan Africa, due to the limited availability of statistical data and household surveys, regarding potential daily and hourly energy usage as well as energy consumption patterns [16]. According to Hasan *et al.* [17], load forecasting models can be divided into four categories: statistical methods, AI methods, knowledge-based expert systems, and hybrids. However, without baseline electrification data, predicting post-electrification energy demand during pre-implementation planning is extremely challenging. As a result, logical village load profiles are often developed using statistical or logical techniques via computer simulations. In mini-grid system design, non-disaggregated hourly time-series power consumption profiles are typically matched with renewable energy generation profiles to achieve system optimization and operational efficiency [16]. However, accurate knowledge of load profiles is essential for determining appropriate component sizing and ensuring optimal initial investment costs.

Several case studies have demonstrated varying approaches to load estimation. In [16], a general load profile analysis method was applied, focusing on differences in loads between weekdays and weekends, as well as seasonal peaks such as those in summer and winter. Seasonal variation was explicitly considered. Similarly, [18] employed an annual load profile analysis to capture year-round variations, also considering seasonal changes. In [19], a Markov Chain Process (stochastic modeling) was used, incorporating socio-economic and gender data to address uncertainty in load behavior. In addition, a study conducted in Oluundje, Namibia, used surveys, interviews, and questionnaires to collect real demand data for hybrid system design. However, it did not explicitly address seasonal variation [20]. In [21], a fixed load forecasting method was used in Amarika, Namibia, assuming a constant daily load across all seasons, thereby not considering seasonal variation. Lastly, [22] focused on institutional loads and employed an empirical load estimation approach. Seasonal variation was considered by differentiating among load types, such as schools and hospitals.

Although various tools and models have been applied to HRES design, most existing approaches still fall short of capturing the full multi-dimensional nature of rural electrification planning. In particular, they rarely integrate cost, reliability, environmental impact, and multi-storage dynamics within a unified optimization framework. These limitations underscore the need for a more comprehensive method capable of jointly exploring the trade-offs among economic, technical, and environmental objectives under varying rural resource conditions.

To address this gap, the present study develops a multi-objective optimization model based on the NSGA-II algorithm to simultaneously minimize *TLCC*, *LCOE*, *LPSP*, *WRE*, and *CO₂* emissions. The proposed framework integrates multiple renewable energy sources (SPV, wind, biomass, and fuel cells) together with complementary storage technologies, including batteries, supercapacitors, and hydrogen storage, enabling robust performance across both transient and steady-state operating conditions.

The novelty of this work lies in the development of an adaptive NSGA-II approach combined with a weighted Pareto based mechanism, allowing systematic evaluation of trade-offs across the five objectives. The model is applied to three rural Namibian communities (Oluundje, Ombudiya, and Onguati), with differing resource availability and load characteristics, demonstrating its scalability, adaptability, and suitability for real-world electrification planning.

MODELING OF RENEWABLE ENERGY AND STORAGE SYSTEMS

The detailed mathematical formulations and simulation procedures for SPV, wind turbines, and biomass gasifiers, along with the corresponding energy storage systems are demonstrated. The models incorporate key environmental, operational, and design parameters to ensure realistic performance evaluation.

Renewable Energy Resources

The following sub-section provides the mathematical models of the different renewable energy systems.

Solar energy. Solar Photovoltaic performance, such as the power output and efficiency, is affected by solar irradiance and ambient temperature [23]. Electricity from SPV is used in many locations [6]; however, due to its intermittent and volatile nature, it is not able to match the time distribution and the load demand [24]. The independent use of SPV results in oversizing, leading to costly, inefficient, and unreliable systems [24].

SPV output power is determined by eq. (1) [23]:

$$P_{pv} = \eta_{pv} A_{pv} G_T [1 - 0.005 (T_c - 25)] \quad (1)$$

where η_{pv} is photoelectric efficiency in (%), A_{pv} is area of the array in (m^2), G_T ($1000 \text{ W}/m^2$) is incident solar radiation, and T_c ($^{\circ}\text{C}$) is cell operation temperature. Global Horizontal Irradiance (GHI) is used for PV G_T . Using GHI and ambient temperature, module temperature is given in eq.(2) [23]:

$$T_c = T_a + \frac{T_{NOCT} - 20}{800} G_T \quad (2)$$

where T_c and T_a denote cell temperature and ambient temperature respectively, and T_{NOCT} is nominal operating cell temperature [23]. T_{NOCT} value is in the range of $45 \pm 3 \text{ }^{\circ}\text{C}$, based on the climate condition of the state [25].

Wind energy. Although wind energy is available throughout the day, it varies geographically, making it location specific [6]. In addition, the availability of the wind resource is intermittent, which leads to technical problems such as power imbalance in the system [26]. Wind turbines with ratings between 0.5 kW and 3 MW are used to extract and convert wind energy into electrical energy. Wind power generation, as given by eq. (3) [27], is affected by factors such as wind speed, air density, wind direction, air pressure, and temperature:

$$P = \begin{cases} P_r, & \text{if } V_r < v(t) < V_{co} \\ P_r \frac{v^3(t) - V_{ci}^3}{V_r^3 - V_{ci}^3}, & \text{if } V_{ci} < v(t) < V_r \\ 0, & \text{if } v(t) \leq V_{ci} \text{ or } v(t) \geq V_{co} \end{cases} \quad (3)$$

where P_r is the rated power, and $v(t)$, V_{ci} , V_{co} , V_r are actual, cut-in, cut-out and rated wind speeds (m/s) respectively. Rated power is defined as a function of the area swept by the wind turbine blades (A_w), air density (ρ_a) (1.225 kg/m³), power coefficient (C_p), and wind turbine generator efficiency (η_g) and rated velocity (V_r) as indicated in eq. (4) [28]:

$$P_r = \frac{1}{2} \rho_a A_w \eta_g C_p V_r^3 \quad (4)$$

Theoretical maximum value of the power coefficient C_p is 0.593, and it is also known as the Betz's coefficient.

Biomass energy. Biomass gasification is a process of partial combustion, in which solid biomass, usually in the form of pieces of wood or agricultural residue is converted into a combustible gas called sync gas [29]. The sizing of the biomass gasifiers is done based on the yearly availability of the feedstock. Moreover, it has been established that biomass is cost effective for mini-grids in villages with greater than 200 households with more than three hours a day of power demand (Pode, Diouf, & Pode, 2015).

Model of a biomass generator is given by eq. (5) and it is used to calculate the power output of the biomass generator [30]:

$$P_{BMG} = \frac{\text{Total fuel wood} \left(\frac{\text{ton}}{\text{yr}} \right) \times \text{Calorific value}_{BM} \times \eta_{BMG} \times 1000}{365 \times 860 \times (\text{operating hours per day})} \quad (5)$$

where η_{BMG} is the efficiency of the biomass generator.

Electrical Energy Storage System

According to Malik *et al.* [31], energy storage is a dominant factor in renewable energy systems, owing to its capability to reduce power fluctuations, enhance system flexibility, and enable effective dispatchability of the electricity generated by variable RESs. Storage technologies are categorised into chemical, electrochemical, mechanical, electromagnetic, and thermal classes, each exhibiting unique performance profiles in lifespan, cost, density, and efficiency. To achieve an optimal storage system, [32] proposed hybridizing two or more storage systems with complementary characteristics to form a Hybrid Energy Storage System (HESS). Mostly, in a HESS, a slow response system is hybridised with fast response systems to achieve higher and improved characteristics.

Mathematical Modeling of the Energy Storage System

The following sub-section provides the mathematical models of the different energy storage systems.

Battery storage system. Eq. (6) is used to model the battery SOC [33]:

$$z(t) = z(t_0) - \frac{1}{Q} \int i(T) d(T) \quad (6)$$

where $z(t)$ is *SOC* at time t , expressed in seconds, $z(t_0)$ is initial *SOC* value, $\frac{1}{Q}$ is battery capacity, and $i(T)$ is current through the battery expressed in [A]. $i(T)$ is positive for the discharging cycle and negative for the charging cycle.

Supercapacitor. Capacitance of the supercapacitor is modeled using eq. (7) [34]:

$$C = \frac{2W}{(0.9 U_R)^3 - (0.7 U_R)^3} \quad (7)$$

where C is capacitance, W is the discharge energy between start and end voltages, and U_R is the rated voltage of the supercapacitor.

Fuel cell. Proton exchange membrane fuel cells (PEMFCs) operate on the electrochemical reaction between hydrogen and oxygen, producing electricity, heat, and water. The mathematical model uses a group of parameters whose definition is essential for the best simulation results [35]. Total output voltage of the fuel cell (FC) is determined by eq. (8):

$$V_{FC} = E_{Nernst} - V_{act} - V_{ohmic} - V_{con} \quad (8)$$

and the voltage of the cells connected in series and forming a stack is determined using eq. (9):

$$V_s = n \times V_{FC} \quad (9)$$

where E_{Nernst} is thermodynamic potential of each unit cell and represents its reversible voltage, V_{act} is voltage drop associated with the activation of the anode and of the cathode, V_{ohmic} is ohmic voltage drop (a measure of the voltage drop associated with the conduction of protons and electrons), V_{con} is voltage drop resulting from the decrease in the concentration of oxygen and hydrogen.

DEVELOPED OBJECTIVE FUNCTION

This study formulates a multi-objective optimization problem for the optimal sizing and integration of hybrid Renewable Energy Systems and Energy Storage Systems (ESSs) to achieve sustainable, reliable, and affordable rural electrification. The problem considers three major categories of objective functions: economic (minimizing the Total Life Cycle Cost (*TLCC*) and *LCOE*), technical (minimizing the *LPSP* and Wasted Renewable Energy (*WRE*)), and environmental (minimizing carbon dioxide (CO_2) emissions). Key decision variables include the capacity sizing of SPV, wind turbines, biomass gasifiers, and storage systems, aiming to ensure an optimal, resilient, and low-carbon microgrid solution for remote communities. Eq. (10) provides the objective function for the study:

$$F(x) = (f_1(x), f_2(x), f_3(x), \dots, f_5(x)) \quad (10)$$

where are:

(a) Financial objectives

$f_1(x)$: Minimise *TLCC*

$f_2(x)$: Minimise *LCOE*

(b) Technical objectives

$f_3(x)$: Minimise *LPSP*

$f_4(x)$: Minimise *WRE*

(c) Environmental objectives:

$f_5(x)$: Minimise total CO_2 emission ($\frac{\text{CO}_2 \text{ emission}}{\text{kg}}$)

Eq. (11) further explains in detail the overall objective function. Objective function: Min (*TLCC, E, LPSP, WRE, CO₂,emission*):

$$\text{Min} \sum_{s=1}^S \left(C_i + \sum_{t=1}^T \frac{(O_t + M_t + F_t)}{(1+r)^t} \right) + \sum_{s=1}^S \left(\frac{I_{\text{cost}} + \sum_{t=1}^T \frac{O_t + M_t(1+g)^{t-1} + F_t}{(1+r)^t}}{\sum_{t=1}^T \frac{E_t}{(1+r)^t}} \right), \frac{\sum_j (P_L(t) - P_{\text{sys,tot}}(t))}{\sum_j (P_L(t))}, \sum_{t=1}^T \frac{P_{\text{wasted}}(t) - P_{\text{sys,tot}}(t)}{P_{\text{sys,tot}}(t)}, \sum_{t=1}^T \text{CO}_{2,\text{emission}} \quad (11)$$

where t is time in years, C_i is initial investment capital, O_t is operational cost with respect to time t , M_t is maintenance cost with respect to time t , F_t is fuel cost with respect to time t , S is energy sources, r is discount rate, g is the annual growth rate of O&M expenditure, E_t is electricity generated in year t , $P_{\text{wasted}}(t)$ is wasted renewable energy in year t , and $P_{\text{sys,tot}}$ is total power of the system.

Equality and Inequalities Constraints

Eq. (12) to (25) define the operational and design constraints necessary for optimizing the HRES. This is to ensure minimized *LPSP*, limit wasted energy, and maintain the state of charge of storage systems (battery and supercapacitor) within safe bounds. The constraints also regulate the sizing of system components, enforce realistic limits on the use of renewable resources, and guarantee the presence of essential system elements like fuel cells and hydrogen storage. Finally, the reliability constraint (shown in eq. (25)) ensures that the system achieves a power supply with *LPSP* above minimum thresholds, thereby prioritizing reliability in rural electrification scenarios.

Power balance equality constraints

$$P_{\text{imb}}(t) = P_L(t) - \left(P_{\text{SPV}}(t) + P_{\text{WG}}(t) + P_{\text{BMG}}(t) + P_{\text{NBAT}}(t) + P_{\text{NSC}}(t) + P_{\text{NFC}}(t) \right) \quad (12)$$

where:

$P_{\text{imb}}(t)$: Is the power imbalance at time t ;

$P_{\text{imb}}(t) > 0$: Demand exceeds supply (deficits);

$P_{\text{imb}}(t) < 0$: Supply exceeds demand (deficit);

$P_{\text{imb}}(t) = 0$: Perfect balance, and where $P_L(t)$, $P_{\text{SPV}}(t)$, $P_{\text{WG}}(t)$, $P_{\text{BMG}}(t)$, $P_{\text{NBAT}}(t)$, $P_{\text{NSC}}(t)$, $P_{\text{NFC}}(t)$, are the load, solar PV, wind generator, biomass generator, battery, and supercapacitor power respectively.

Wasted power equalities constraints

$$P_{SPV}(t) + P_{WG}(t) - (P_L(t) + P_{BAT,stor}(t) + P_{SC,stor}(t)) = P_{wasted}(t) \quad (13)$$

$$P_{wasted}(t) = \frac{P_{wasted}(t) - P_{syst,tot}}{P_{syst,tot}} \quad (14)$$

where $P_{syst,tot}$ is total power.

Storage system operational inequality constraints

$$SOC_{BAT,MIN}(t) \leq SOC_{BAT} \leq SOC_{BAT,MAX} \quad (15)$$

$$SOC_{SC,MIN}(t) \leq SOC_{SC} \leq SOC_{SC,MAX} \quad (16)$$

$$L_{H_2,storage}(t) > 0 \quad (17)$$

where $SOC_{BAT,MIN}(t)$, SOC_{BAT} , $SOC_{BAT,MAX}(t)$, is the minimum, actual and maximum battery state of charge with respect to time. $SOC_{SC,MIN}(t)$, SOC_{SC} , $SOC_{SC,MAX}(t)$, is the minimum, actual and supercapacitor state of charge and $L_{H_2,storage}(t)$ is the level of hydrogen in the hydrogen storage tank (%).

Renewable energy inequalities constraint

$$C_{SPV} \geq 0 \quad (18)$$

$$C_{WG} \geq 0 \quad (19)$$

$$C_{BMG} \geq 0 \quad P_{BMG} \leq P_{BMG,MAX} \text{ (Biomass resources)} \quad (20)$$

where C_{SPV} , C_{WG} , C_{BMG} are SPV, wind and biomass generator capacity respectively. P_{BMG} and $P_{BMG,MAX}$ are the optimized biomass power capacity and maximum ideal power respectively.

Storage sizing inequities constraint

$$C_{BAT} \geq 0 \quad (21)$$

$$C_{SC} \geq 0 \quad (22)$$

$$C_{FC} \geq 0 \quad (23)$$

$$C_{H_2,storage} \geq 0 \quad (24)$$

where C_{BAT} , C_{SC} , C_{FC} , $C_{H_2,storage}$ are the battery, supercapacitor, fuel cell, and hydrogen storage capacity respectively.

Reliability equality constraint

$$LPSP \leq 0.5 \quad (25)$$

PROPOSED OPTIMIZATION ALGORITHM

The following sub-section provides the proposed optimization algorithm adapted in the study.

Selection of Energy Storage Systems

Considering the intermittency of the RESs and fluctuation of load demand, there is a need for short-term storage to regulate the power quality and ensure balance between demand and generation at all times. Moreover, it is pertinent to ensure a continuous steady state power supply when the power generated is insufficient to meet the load demand. Based on the analysis of the different storage technologies, the supercapacitor, battery, and hydrogen storage technologies have been considered in this study for analysis in terms of their transient and steady state responses as described below:

- (i) **Supercapacitors** have the highest power density, instantaneous response, and higher lifespan. Therefore, they are used for the transient response to counter act the dynamic fluctuation of the RESs and the load demand and remove stress from the BESSs thus prolonging their lifespan.
- (ii) **Batteries** have high power and energy density, fast response, and low operating cost. Therefore, they will be used for both transient and steady state responses to cater to periods when the generation from the RESs is lower or greater than the load demand power.
- (iii) **Fuel Cell (Hydrogen)**: Hydrogen has the highest energy density, zero self-discharge, and long-term storage application. Therefore, this storage system will be used to cater for steady state responses for long periods of lower generation from the RESs.

Optimization Algorithm Approach

Figure 1 outlines the steps taken in developing the proposed algorithm, NSGA-II, which is a widely adopted multi-objective evolutionary algorithm designed to identify a diverse set of Pareto-optimal solutions for problems with conflicting objectives [14]. Initialization of a randomly generated population of candidate solutions is carried out, each evaluated against predefined objective functions such as minimizing *TLCC*, *LCOE*, *LPSP*, and *CO₂* emissions. Non-dominated sorting is then applied to rank solutions into different fronts based on Pareto dominance, where the best (non-dominated) forms the first front, followed by the second front, and so forth. To maintain diversity among solutions, a crowding distancing is determined for each individual within a front. Pareto solutions are selected using a binary tournament selection mechanism that considers both rank and crowding distance. These undergo genetic operations, typically simulated binary crossover (SBX) and polynomial mutation to generate offspring [15]. The iterative process continues until a predefined stopping criterion is reached, ultimately producing a Pareto-optimal front that offers systems planners multiple trade-off solutions across economic, technical, and environmental objectives.

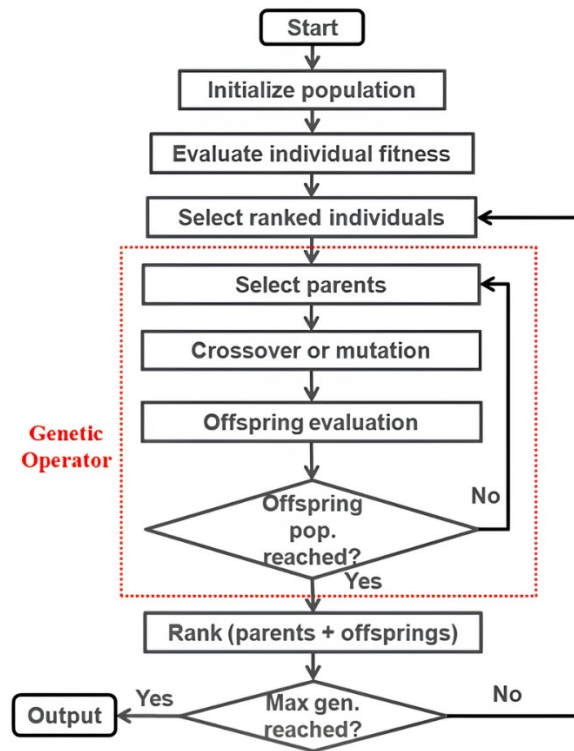


Figure 1. NSGA-II algorithm flowchart (Chang, Bouzarkouna, & Devegowda, 2015)

ENERGY MANAGEMENT STRATEGY

The proposed Energy Management System (EMS), illustrated in [Figure 2](#), is designed to mitigate RESs intermittency and load variability, ensuring a continuous and reliable power supply. It integrates real-time data from PV and wind sources, monitors the state of charge (SOC) of storage systems, and dynamically regulates charge-discharge actions for optimal component performance. Hydrogen tank levels are tracked to coordinate fuel cell operation, while a load-following strategy enables the fuel cell and biomass generator to adjust output in line with demand.

Weighted Optimal Solution Criteria

Pareto optimal configurations obtained from the optimization process are ranked using a weighted approach, where each objective function is assigned a normalized weight (0 – 1) for computation. The configuration with the highest total score is selected as the best option. The weighting factors are 0.35 for *LCOE*, 0.35 for reliability (*LPSP*), 0.10 for emission, and 0.20 for wasted power, reflecting the prioritization of cost and reliability in rural electrification projects.

Selected Renewable Energy Sources

Integrating multiple energy sources for sustainable power supply has proven to be a challenge due to the variability and intermittence nature of the RESs, leading to generation uncertainty. Although Solar and wind are non-dispatchable and not recommended as base-load sources, they are more abundant, clean, and inexhaustible as compared to biomass, which depends on feedstock availability (Baloyi, Kibaara, & Chowdhury, 2016). It has been established that Biomass systems have *LCOE* values of 0.11 – 0.28 USD/kWh [6], while mini-hydropower can achieve 0.05 USD/kWh [36]. Hydropower, though renewable, is not considered in this study due to the scarcity of water resources in Namibia’s rural areas.

Renewable Energy Resources Assessment

A preliminary assessment, based on cartographic surveys, prospecting methods, and literature reviews identified solar, wind, and biomass (encroacher bush) as viable resources for rural electrification in Namibia. Three unelectrified rural areas, Onguati (Kunene region), Ombundiya (Ohangwena region), and Oluundje (Oshikoto region) were selected to represent low, high, and average resource availability, respectively. Population density was also a selection criterion. Resource and load data from these sites were used for model verification and validation. The geographical location of the three rural areas is provided in [Table 1](#).

Table 1. The geographical location of the three selected rural areas

Village name	Latitude	Longitude	Region	Part of the country
Oluundje	-18.01	16.74	Oshikoto	Northern part
Ombudiya	-17.43	17.33	Ohangwena	Northern Part
Onguati	-19.80	14.54	Kunene	Western Part

Resource analysis utilised data from the NASA NERRA-2 database at 50 m height. Namibia has four seasons, but only summer and winter were analysed due to their dominant influence on resource variation. Seasonal diurnal analysis of solar irradiance and wind speed was performed to evaluate variability.

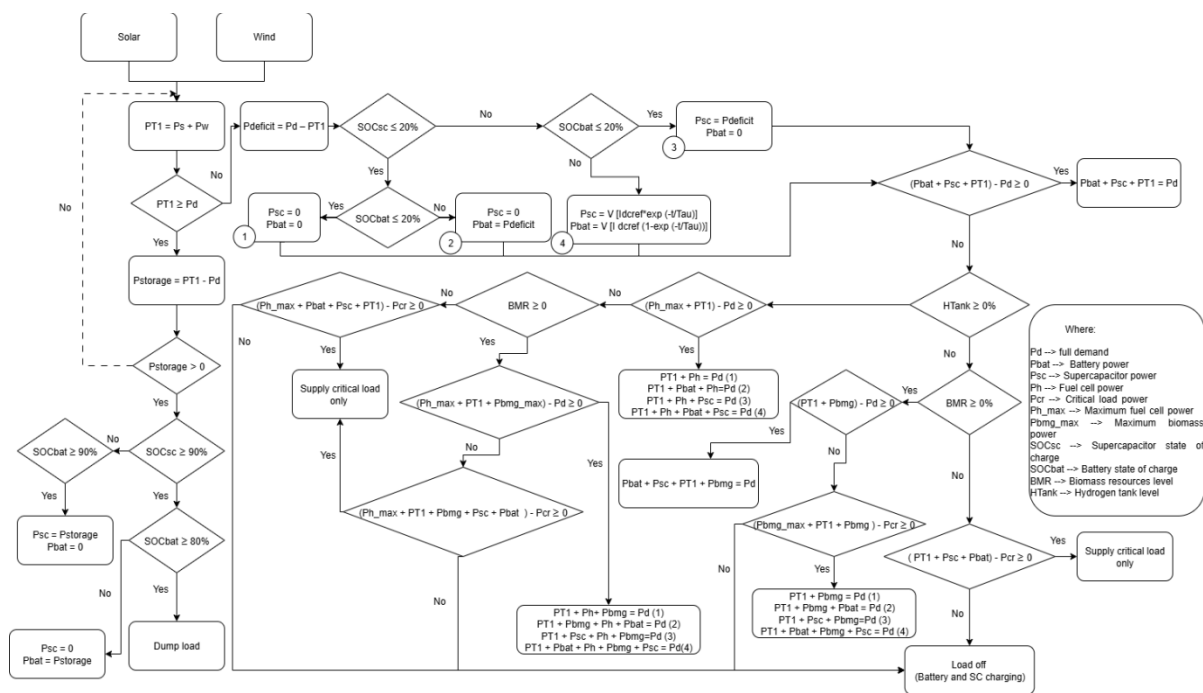


Figure 2. Energy management flowchart

Solar Irradiance. [Figure 3](#) to [Figure 5](#) show diurnal solar irradiance for the three sites. Solar energy is available mainly between 06:00 and 18:00, peaking between 11:00 and 12:00, with no irradiance from 19:00 to 05:00. Seasonal variations in irradiance and sunshine hours were observed across sites, but all locations recorded daily global horizontal irradiance (*GHI*) above the 4.4 kWh/m²/day threshold, indicating suitability for solar power development.

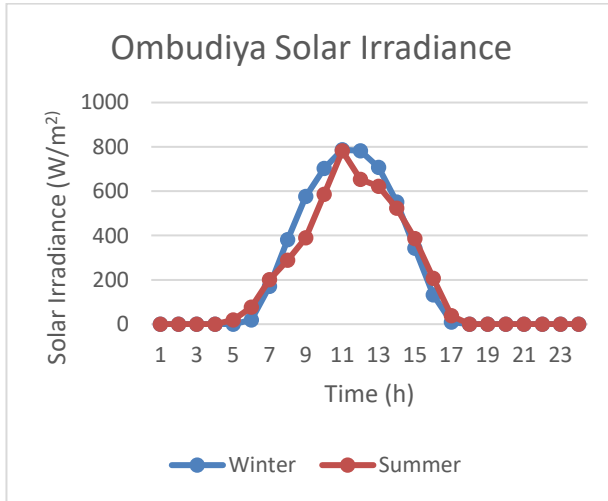


Figure 3. Winter and summer diurnal solar irradiance for Ombudiya village

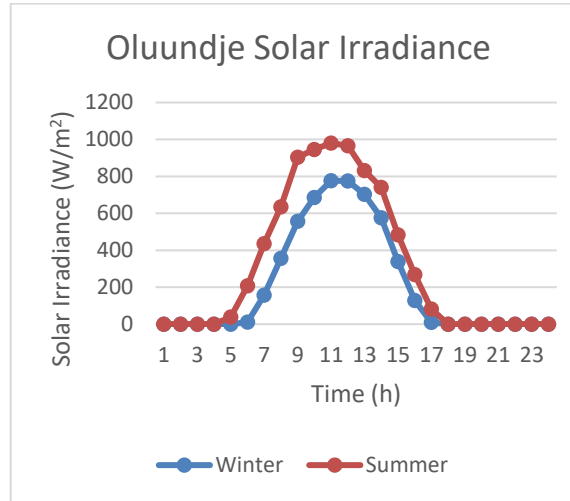


Figure 4. Winter and summer diurnal solar irradiance for Oluundje village

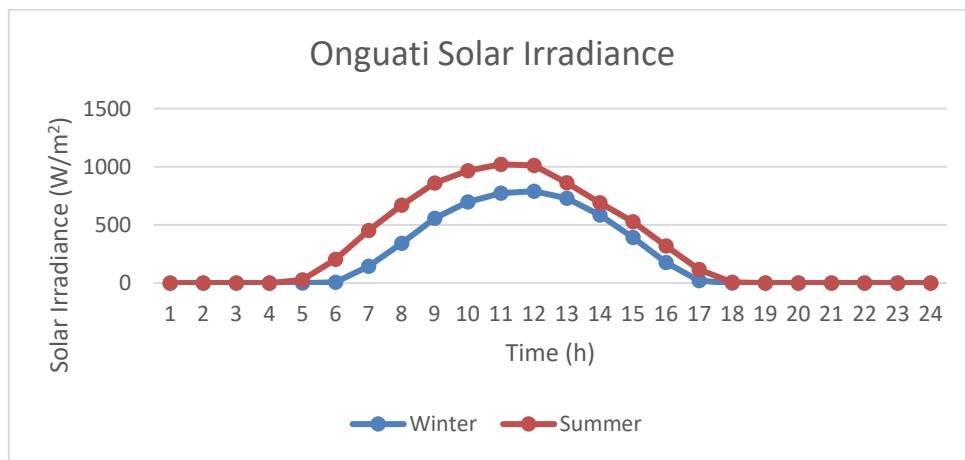


Figure 5 Winter and summer diurnal solar irradiance for Onguati village

Biomass Resource. Table 2 shows the power generation of the selected sites using biomass. It can be seen that Oluundje and Ombudiya have higher resources compared to Onguati. This plays a significant role in hybrid configurations as will be shown in the upcoming sections.

Table 2. Biomass resources of the three rural areas

Village	Area (ha)	Resource (dry tonnes/year)	Resource (kWh/year) (only 30% of resource)
Oluundje	2342	1011.74	1518346.2
Ombudiya	3038.8	1312.76	1969140
Onguati	4663.6	91.58	137370

Wind Speed. Figure 6 to Figure 8 illustrate seasonal diurnal wind speed variations. Oluundje and Ombudiya experience their highest wind speeds during winter nights, while Onguati records peak wind speeds in summer afternoons, with lower speeds in mornings and at night. This temporal and seasonal variability influences the contribution of wind power within each village’s hybrid system.

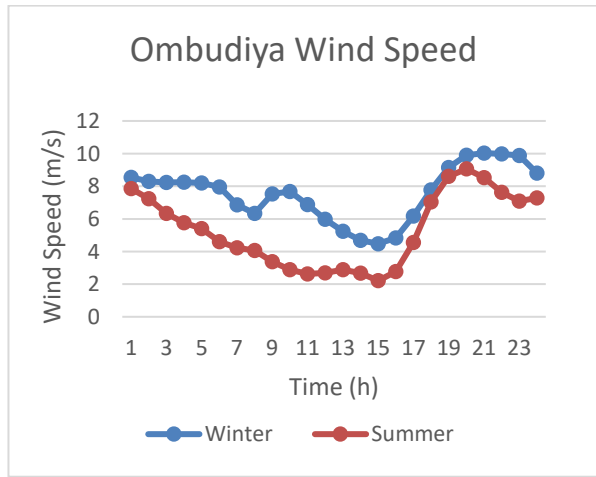


Figure 6. Winter and summer diurnal wind speed for Ombudiya village

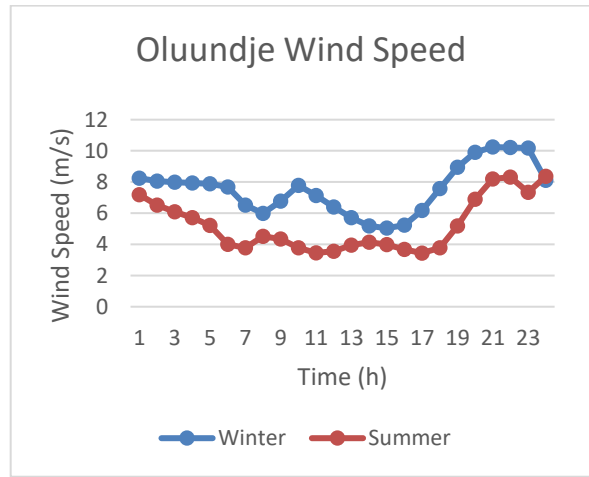


Figure 7. Winter and summer diurnal wind speed for Oluundje village

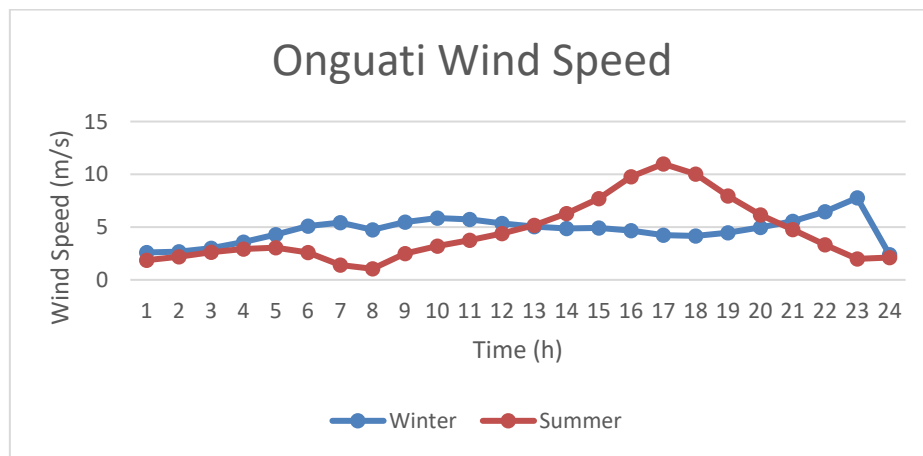


Figure 8. Winter and summer diurnal wind speed for Onguati village

Proposed Load Estimate Algorithm

A bottom-up probabilistic approach was applied for load modelling to capture demand uncertainty and growth, supported by survey data and government policy. While appliance types and usage patterns were standardised across the three villages due to similar socio-economic conditions, the number of households varied as given in Table 3.

Table 3. The estimated number of households in each selected rural area

Rural Area	Total Area (km)	Population density(person/km)	Total population (Total Area×Population density)	Average number of person per room (3 rooms per house)	Number of households
Oluundje	32.27	26.7	862	1.2	240
Onguati	46.92	3.8	179	2.1	29
Ombudiya	34.24	31.7	1086	1.3	279

Adapted load demand forecasting algorithm. Models used in forecasting load demand is as described by eq. (26) and eq. (27):

$$D_h = \sum_j^{\text{Userclass}} N_j \sum_i^{\text{Appliance}} n_{ij} P_{ij} \tag{26}$$

$$D_d = \sum_{h=0}^{23} D_h \tag{27}$$

where h is the hour of the day [$h=0,1,2,3,\dots,23$], i refers to the type of electrical appliances and refers to the type of consumer, N_j is the number of users and n_{ij} is the type of appliance of each consumer class (TVs, lights, phones, etc.), P_{ij} represents the nominal power of the different types of appliances of each consumer, D_d is the total daily load demand of the entire system, D_h is the hourly load demand of the entire system.

Total forecasted load demand. For the modeling process, it was assumed that each village contains one clinic, one school, one church, and a specified number of shops: 15 for Oluundje and Ombudiya, and 2 for Onguati. **Figure 9** illustrates the detailed daily load demand distribution for each village

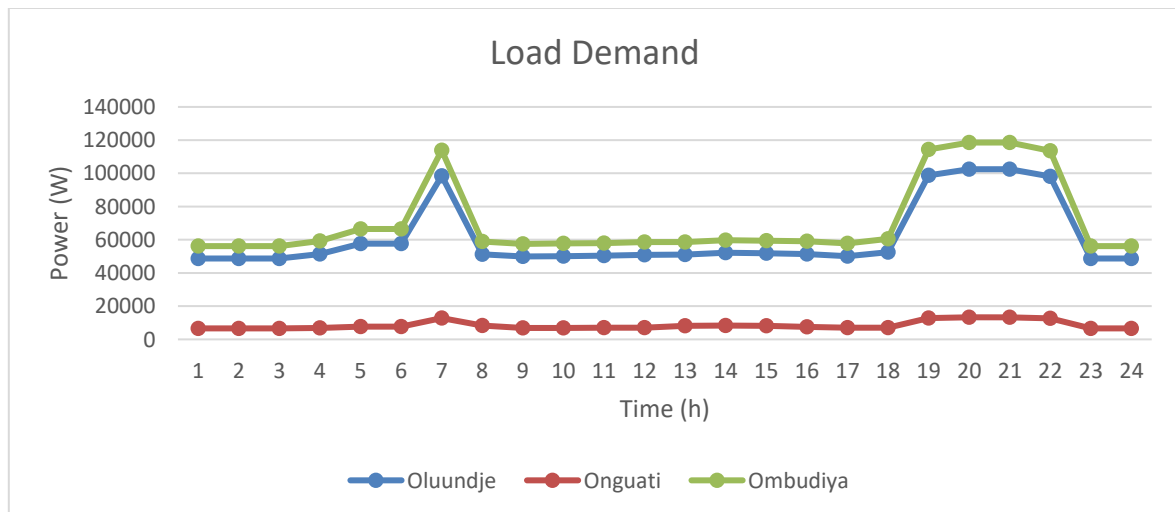


Figure 9. Daily disaggregated load demand of the three rural villages

OPTIMIZATION RESULTS AND ANALYSIS

The following sub-section provides optimization results and analysis.

Optimal Solution

The optimization process considered 10 generations and a population size of 10. **Figure 10** to **Figure 18** depict Pareto-optimal solutions, with the best selected configurations highlighted with a red rectangle. In Oluundje and Ombudiya, biomass was dominant in the best solutions, yielding minimum *LCOE* values. In Onguati, limited biomass availability led to a wind-dominated configuration with reduced storage requirements.

Oluundje village

paretofront						
LCOE/kWh	TLCC	Reliability	Emissionst...	WastedPo...	CapacitieskW	
Number	Number	Number	Number	Number	Text	
LCOE (\$/kW...	TLCC (\$)	Reliability	Emissions (t...	Wasted Po...	Capacities (kW)	
1	0.3453	390357.00	1.28%	3015.73	38842.86	battery: 12.62, biomass: 0.00, fuel_cell: 12.00, hydrogen_budget: 13759.11, solar: 26.01, super_capacitor: 0.82, wind: 40.94
2	0.2098	419310.00	17.88%	5923.80	116162.68	battery: 168.03, biomass: 0.00, fuel_cell: 30.00, hydrogen_budget: 5867.82, solar: 60.97, super_capacitor: 3.92, wind: 13.80
3	0.3521	517190.00	37.88%	18522.84	346542.21	battery: 114.49, biomass: 0.00, fuel_cell: 18.00, hydrogen_budget: 5867.82, solar: 196.09, super_capacitor: 6.85, wind: 6.46
4	0.0015	602133.00	100.00%	90583327.86	102964.19	battery: 15.02, biomass: 200.00, fuel_cell: 30.00, hydrogen_budget: 40124.13, solar: 25.50, super_capacitor: 6.85, wind: 35.23
5	0.0042	849173.00	99.28%	45295142.08	283482.47	battery: 180.93, biomass: 100.00, fuel_cell: 60.00, hydrogen_budget: 34314.05, solar: 26.10, super_capacitor: 2.56, wind: 177.09
6	0.3008	1072327.00	56.19%	43589.68	1058227.74	battery: 102.24, biomass: 0.00, fuel_cell: 60.00, hydrogen_budget: 28912.64, solar: 447.38, super_capacitor: 2.48, wind: 110.22
7	0.0033	1307743.00	100.00%	90620993.95	1138339.64	battery: 123.11, biomass: 200.00, fuel_cell: 60.00, hydrogen_budget: 43850.88, solar: 407.34, super_capacitor: 6.85, wind: 162.43
8	0.4969	1499070.00	88.33%	43656.54	1254462.76	battery: 179.78, biomass: 0.00, fuel_cell: 48.00, hydrogen_budget: 14620.36, solar: 408.63, super_capacitor: 3.51, wind: 376.34
9	0.0084	1704141.00	99.87%	45333876.54	1410282.63	battery: 179.78, biomass: 100.00, fuel_cell: 96.00, hydrogen_budget: 67895.58, solar: 408.63, super_capacitor: 4.33, wind: 376.34
10	0.5206	647231.00	40.24%	19103.33	361281.46	battery: 113.68, biomass: 0.00, fuel_cell: 12.00, hydrogen_budget: 8086.44, solar: 190.29, super_capacitor: 9.64, wind: 87.22

Figure 10. Pareto optimal solutions (Oluundje village)

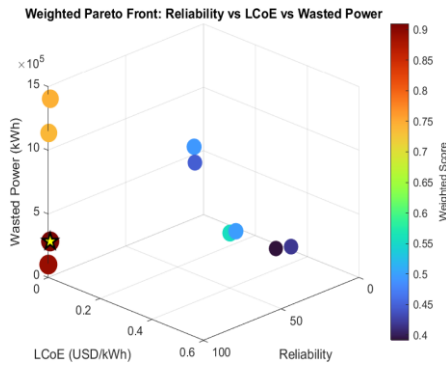


Figure 11. Oluundje village Pareto optimal graph

```
Results exported to ./documents/pareto_front.csv
ParetoEvaluation initialized!
Weighted Score: 0.4182, LCOE: 0.3453
Weighted Score: 0.5571, LCOE: 0.2098
Weighted Score: 0.4985, LCOE: 0.3521
Weighted Score: 0.8907, LCOE: 0.0015
Weighted Score: 0.9100, LCOE: 0.0042
Weighted Score: 0.4942, LCOE: 0.3008
Weighted Score: 0.7385, LCOE: 0.0033
Weighted Score: 0.4473, LCOE: 0.4969
Weighted Score: 0.7449, LCOE: 0.0084
Weighted Score: 0.3911, LCOE: 0.5206
```

Figure 12. Oluundje village weighted Pareto optimal solutions

Onguati village

paretofront						
LCOE/kWh	TLCC	Reliability	Emissionst...	WastedPo...	CapacitieskW	
Number	Number	Number	Number	Number	Text	
LCOE (\$/kW...	TLCC (\$)	Reliability	Emissions (t...	Wasted Po...	Capacities (kW)	
1	0.1193	79300.00	81.24%	416.99	12623.19	battery: 108.49, biomass: 0.00, fuel_cell: 12.00, hydrogen_budget: 43172.94, solar: 4.22, super_capacitor: 0.77, wind: 5.68
2	0.0783	122500.00	44.58%	416.99	13565.51	battery: 187.40, biomass: 0.00, fuel_cell: 30.00, hydrogen_budget: 27363.01, solar: 4.22, super_capacitor: 0.92, wind: 5.68
3	0.0328	467111.00	100.00%	3005025.41	495524.83	battery: 191.08, biomass: 100.00, fuel_cell: 24.00, hydrogen_budget: 33502.17, solar: 230.61, super_capacitor: 0.96, wind: 23.92
4	0.0811	784142.00	94.20%	2335.91	162484.52	battery: 154.21, biomass: 0.00, fuel_cell: 192.00, hydrogen_budget: 4472.54, solar: 8.68, super_capacitor: 3.10, wind: 149.64
5	0.0540	1141124.00	100.00%	3006997.79	674929.53	battery: 221.70, biomass: 100.00, fuel_cell: 162.00, hydrogen_budget: 27363.01, solar: 230.61, super_capacitor: 6.77, wind: 207.93
6	0.1095	1550400.00	100.00%	6747.63	473315.53	battery: 430.01, biomass: 0.00, fuel_cell: 282.00, hydrogen_budget: 49676.47, solar: 24.57, super_capacitor: 6.77, wind: 436.14
7	0.0589	2042141.00	100.00%	3028383.20	1192154.21	battery: 209.43, biomass: 100.00, fuel_cell: 432.00, hydrogen_budget: 44421.68, solar: 484.90, super_capacitor: 6.77, wind: 201.95
8	0.0572	2188260.00	100.00%	3028229.68	1178420.17	battery: 234.40, biomass: 100.00, fuel_cell: 504.00, hydrogen_budget: 84062.10, solar: 484.90, super_capacitor: 2.02, wind: 187.63
9	0.7370	727257.00	100.00%	48418.65	1178752.59	battery: 139.56, biomass: 0.00, fuel_cell: 18.00, hydrogen_budget: 8707.17, solar: 570.19, super_capacitor: 3.07, wind: 30.18
10	0.7658	756189.00	100.00%	48585.16	1193242.78	battery: 76.85, biomass: 0.00, fuel_cell: 18.00, hydrogen_budget: 73653.33, solar: 570.19, super_capacitor: 2.05, wind: 45.72

Figure 13. Pareto optimal solutions (Onguati village)

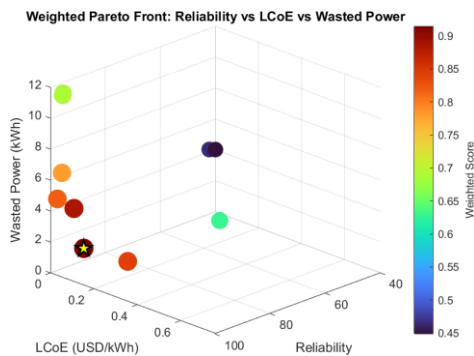


Figure 14. Pareto optimal graph (Onguati village)

```
Results exported to ./documents/pareto_front.csv
ParetoEvaluation initialized!
Weighted Score: 0.8402, LCOE: 0.1193
Weighted Score: 0.6281, LCOE: 0.0783
Weighted Score: 0.8190, LCOE: 0.0328
Weighted Score: 0.9148, LCOE: 0.0811
Weighted Score: 0.7784, LCOE: 0.0540
Weighted Score: 0.8851, LCOE: 0.1095
Weighted Score: 0.6877, LCOE: 0.0589
Weighted Score: 0.6909, LCOE: 0.0572
Weighted Score: 0.4646, LCOE: 0.7370
Weighted Score: 0.4484, LCOE: 0.7658
```

Figure 15. Weighted Pareto optimal solutions (Onguati village)

Ombudiya village

paretofront						
LCOEkWh	TLCC	Reliability	Emissionst...	WastedPo...	CapacitieskW	
Number	Number	Number	Number	Number	Text	
LCOE (\$/kWh)	TLCC (\$)	Reliability	Emissions (t)	Wasted Po	Capacities (kW)	
1	0.3922	348888.00	0.00%	2266.01	0.00	battery: 21.70, biomass: 0.00, fuel_cell: 6.00, hydrogen_budget: 1149.67, solar: 23.12, super_capacitor: 0.07, wind: 6.75
3	0.2264	395741.00	0.00%	1150.84	23044.54	battery: 16.26, biomass: 0.00, fuel_cell: 24.00, hydrogen_budget: 683.07, solar: 9.86, super_capacitor: 0.41, wind: 16.10
4	0.0023	445091.00	79.82%	45293040.91	74952.55	battery: 40.86, biomass: 100.00, fuel_cell: 6.00, hydrogen_budget: 2186.42, solar: 29.01, super_capacitor: 0.02, wind: 6.86
5	0.0026	509010.00	80.15%	45293055.29	86426.90	battery: 97.97, biomass: 100.00, fuel_cell: 24.00, hydrogen_budget: 2966.95, solar: 27.37, super_capacitor: 0.02, wind: 18.89
6	0.0999	592830.00	0.65%	742.47	29393.82	battery: 6.71, biomass: 0.00, fuel_cell: 108.00, hydrogen_budget: 3230.95, solar: 5.51, super_capacitor: 0.01, wind: 16.10
7	0.0044	874690.00	84.05%	45325762.03	884224.18	battery: 120.33, biomass: 100.00, fuel_cell: 24.00, hydrogen_budget: 3837.50, solar: 375.11, super_capacitor: 0.01, wind: 21.29
8	0.4392	1229391.00	52.49%	45277.88	1112608.91	battery: 6.19, biomass: 0.00, fuel_cell: 42.00, hydrogen_budget: 1156.04, solar: 453.23, super_capacitor: 1.90, wind: 193.18
9	0.5470	723539.00	41.66%	33341.00	633860.24	battery: 64.75, biomass: 0.00, fuel_cell: 12.00, hydrogen_budget: 407.70, solar: 352.40, super_capacitor: 0.41, wind: 16.52
10	0.5872	777844.00	41.37%	39475.17	774279.33	battery: 16.32, biomass: 0.00, fuel_cell: 12.00, hydrogen_budget: 426.43, solar: 418.86, super_capacitor: 0.13, wind: 8.61
11	0.6560	897099.00	42.63%	40367.54	812511.26	battery: 16.26, biomass: 0.00, fuel_cell: 12.00, hydrogen_budget: 460.58, solar: 418.86, super_capacitor: 0.31, wind: 72.62

Figure 16. Pareto optimal solutions (Ombudiya village)

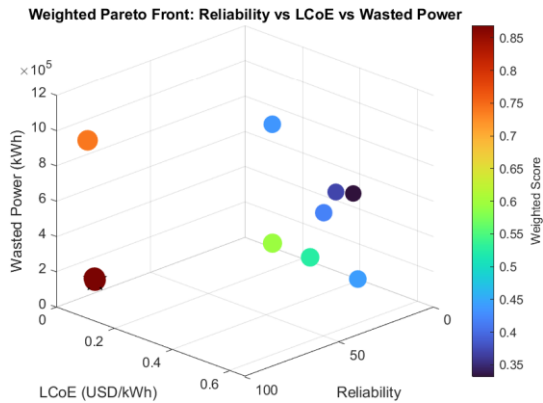


Figure 17. Pareto optimal graph (Ombudiya village)

```

Results exported to ./documents/pareto_front.csv
ParetoEvaluation initialized!
Weighted Score: 0.4412, LCOE: 0.3922
Weighted Score: 0.5259, LCOE: 0.2264
Weighted Score: 0.8690, LCOE: 0.0023
Weighted Score: 0.8681, LCOE: 0.0026
Weighted Score: 0.5951, LCOE: 0.0999
Weighted Score: 0.7399, LCOE: 0.0044
Weighted Score: 0.4345, LCOE: 0.4392
Weighted Score: 0.4178, LCOE: 0.5470
Weighted Score: 0.3698, LCOE: 0.5872
Weighted Score: 0.3314, LCOE: 0.6560
    
```

Figure 18. Weighted Pareto optimal solutions (Ombudiya village)

Power Flow Charts

Figure 19 to Figure 27 present hourly and seasonal power profiles for the selected optimal configurations. Oluundje and Ombudiya rely on biomass as a dispatchable resource to bridge gaps during periods of low renewable output, while Onguati depends predominantly on wind and solar, supported by energy storage in the form of supercapacitors and batteries. This seasonal complementarity, with stronger winds in winter and higher solar output in summer, helps maintain a balanced, year-round power supply.

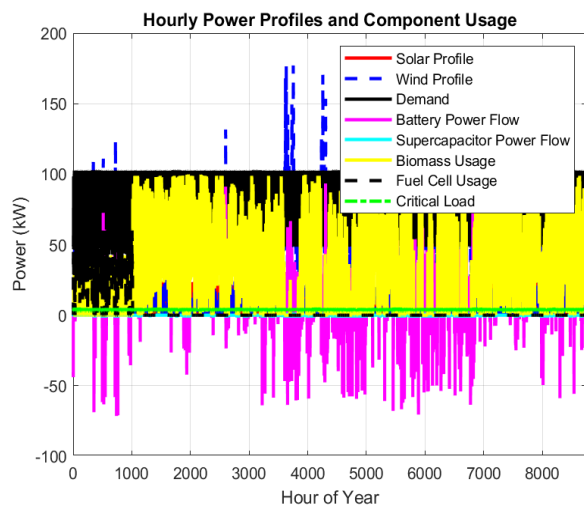


Figure 19. Hourly power profile (Oluundje village)

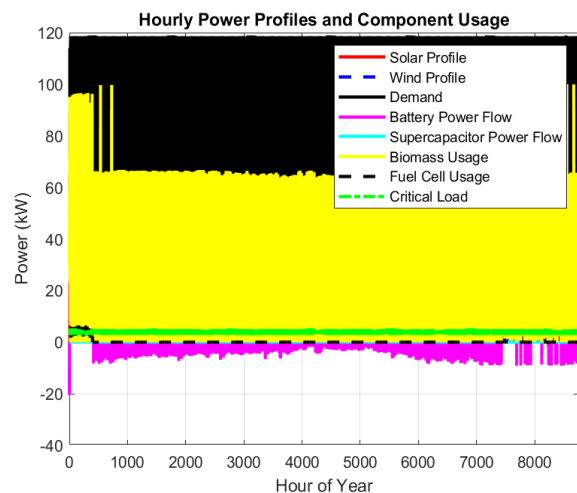


Figure 20. Ombudiya village hourly power profile

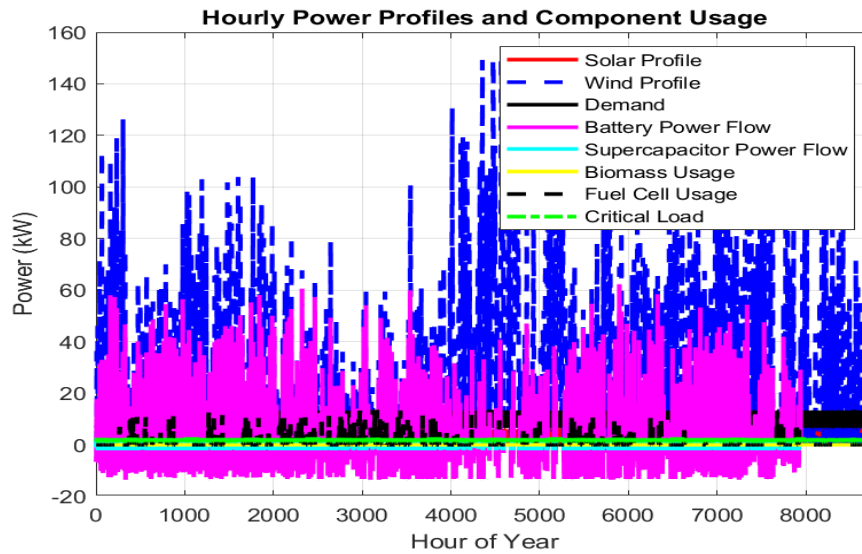


Figure 21. Village hourly power profile (Onguati)

Oluundje village

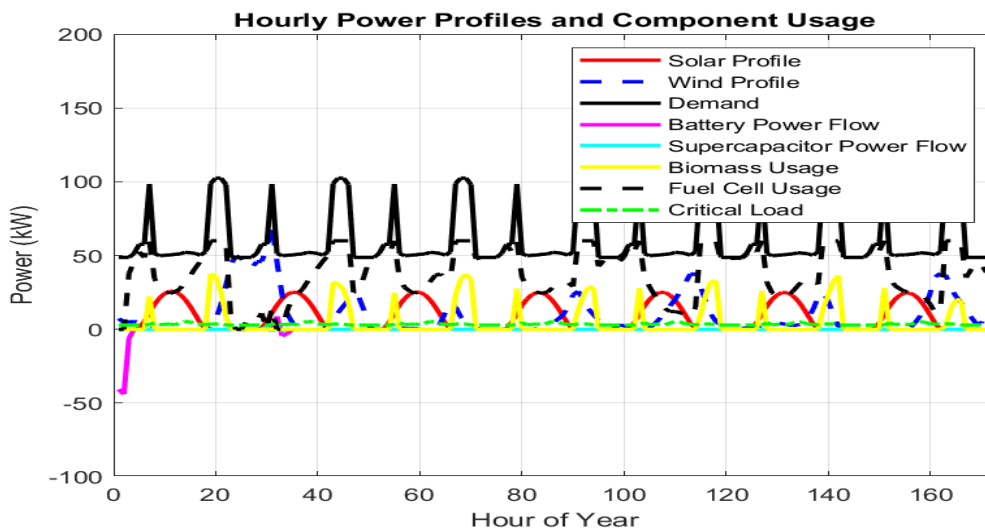


Figure 22. Hourly power profiles and component usage for Oluundje village during summer

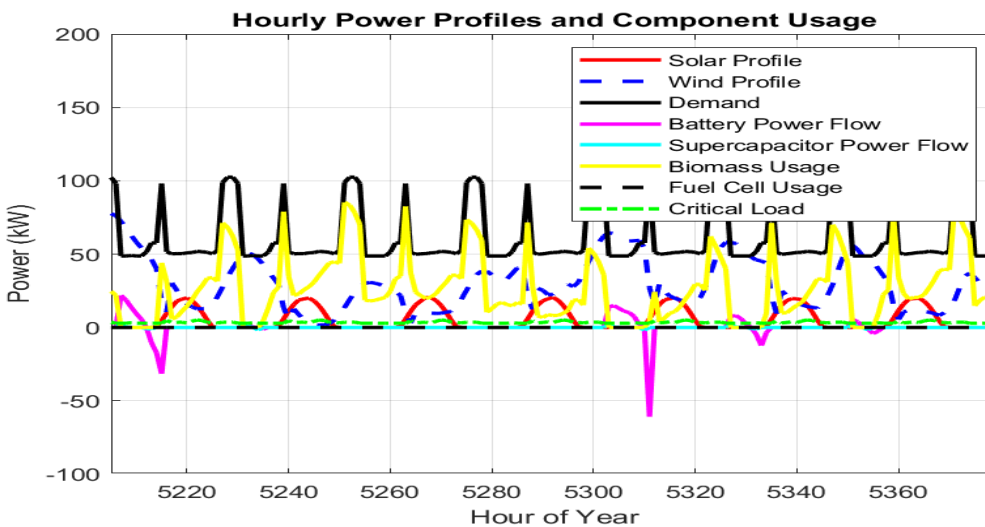


Figure 23. Hourly power profiles and component usage for Oluundje village during winter

Ombudiya village

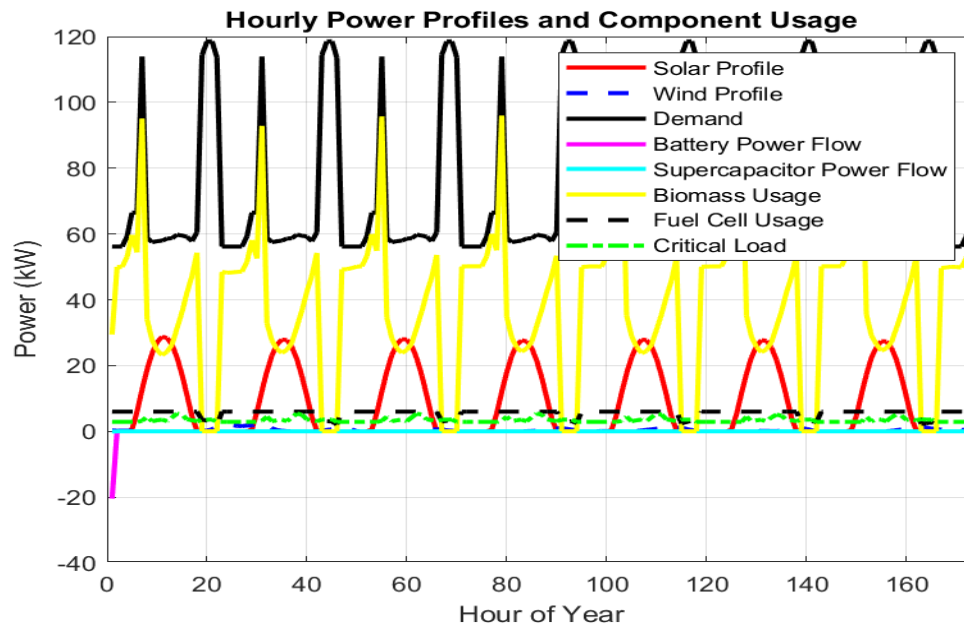


Figure 24. Hourly power profiles and component usage for Ombudiya village during summer

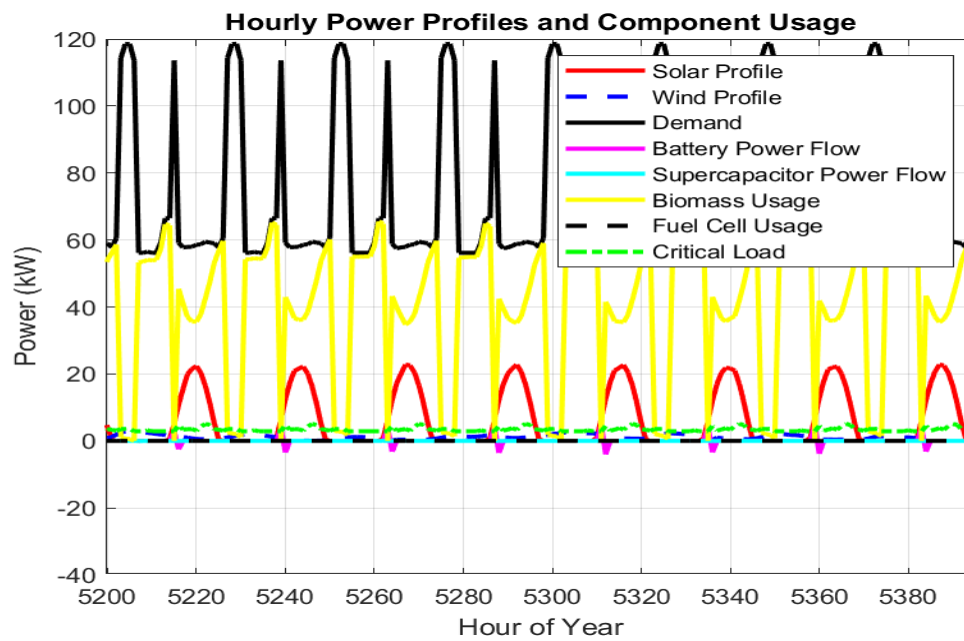


Figure 25. Hourly power profiles and component usage for Ombudiya village during winter

Onguati village

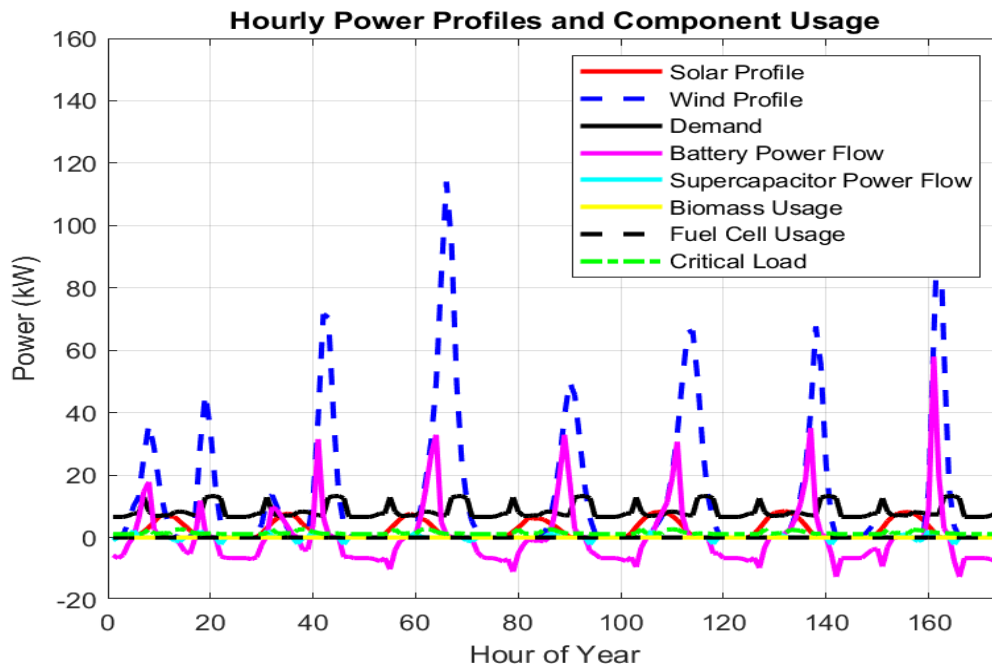


Figure 26. Hourly power profiles and component usage for Onguati village during summer

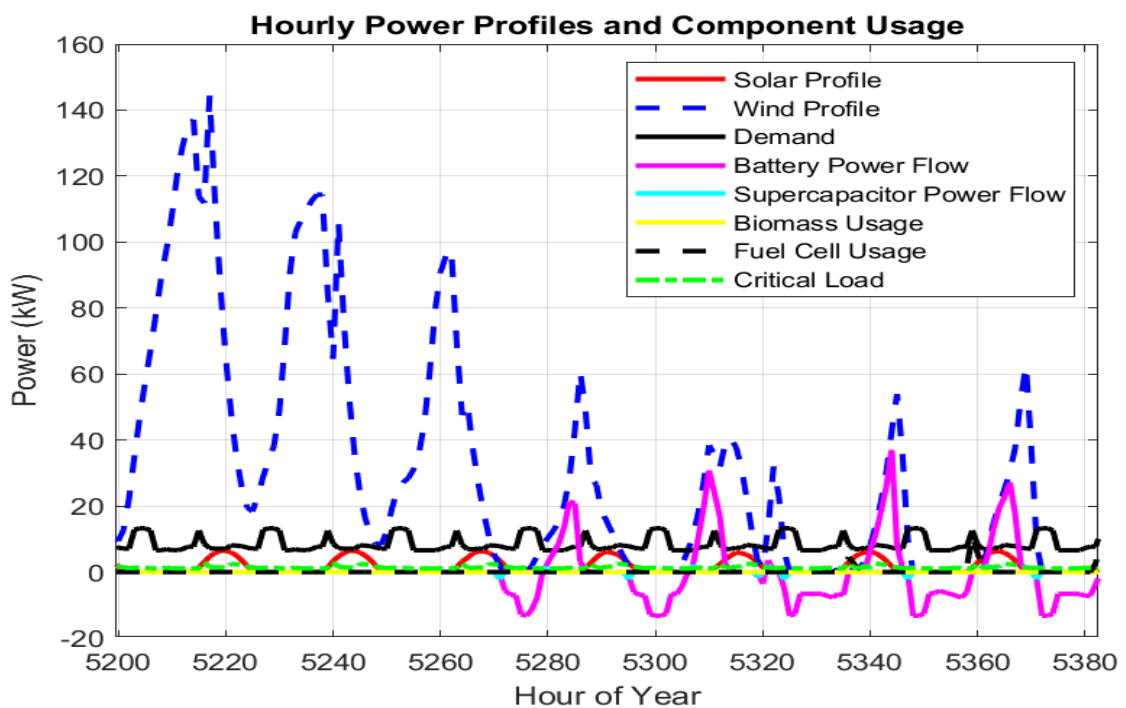


Figure 27. Hourly power profiles and component usage for Onguati village during winter

Energy Storage Flowcharts

Figure 28 to Figure 33 show State-of-Charge (SOC) cycles for batteries and supercapacitors alongside biomass and hydrogen budgets. Storage cycling is minimal in Oluundje and Ombudiya due to biomass dispatchability. In Onguati, frequent storage cycling occurs due to reliance on non-dispatchable sources. Biomass depletion is gradual in villages where it is used, while hydrogen fuel cells serve as immediate backup when renewables and storage are insufficient.

Oluundje village

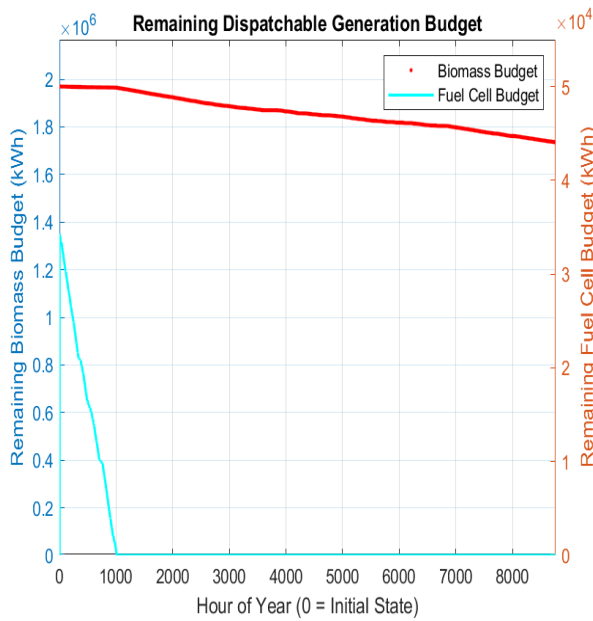


Figure 28. Remaining dispatchable generation budget for Oluundje village throughout the year

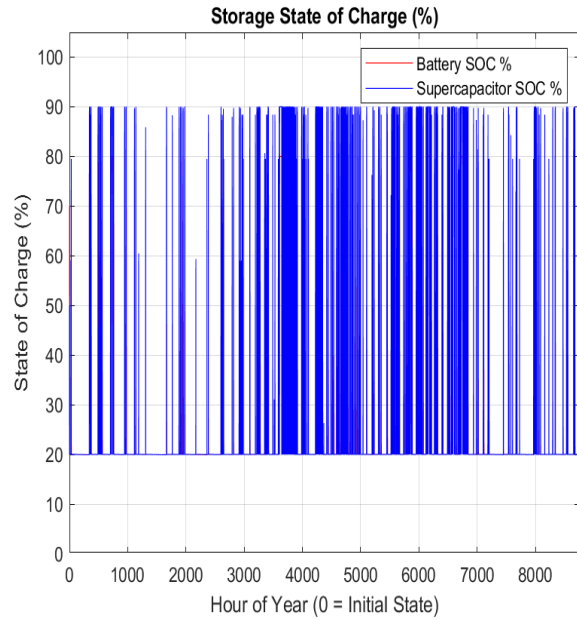


Figure 29. Battery and supercapacitor state-of-charge trends for Oluundje village throughout the annual operation

Ombudiya village

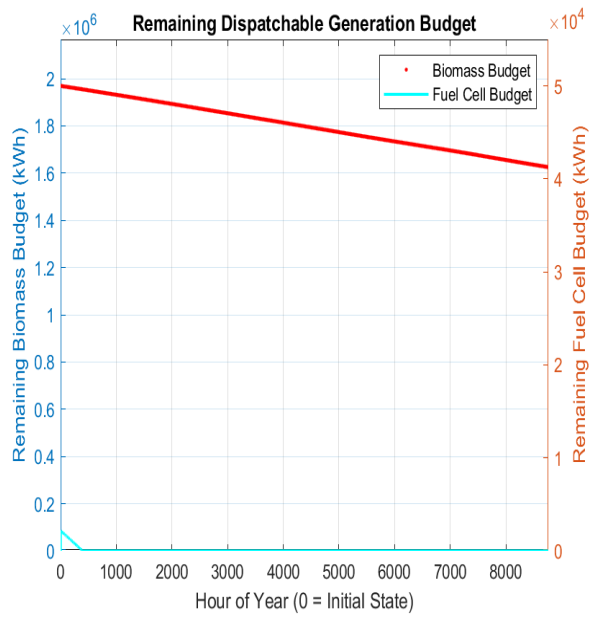


Figure 30. Remaining dispatchable generation budget for Ombudiya village throughout the year

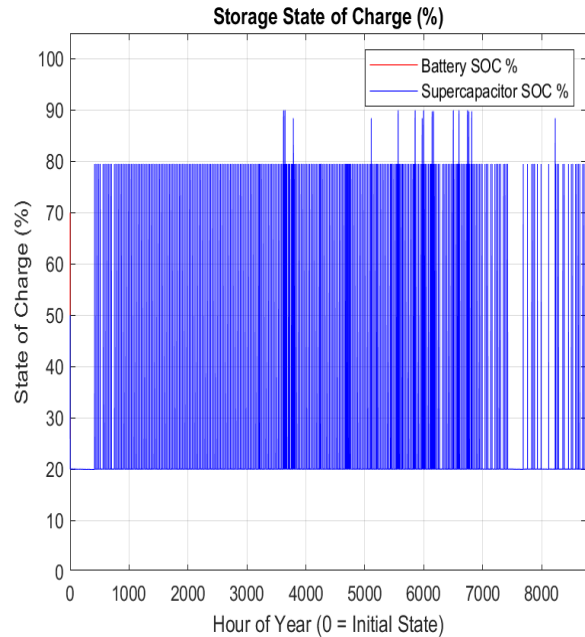


Figure 31. Battery and supercapacitor state-of-charge trends for Ombudiya Village throughout the annual operation

Onguati village

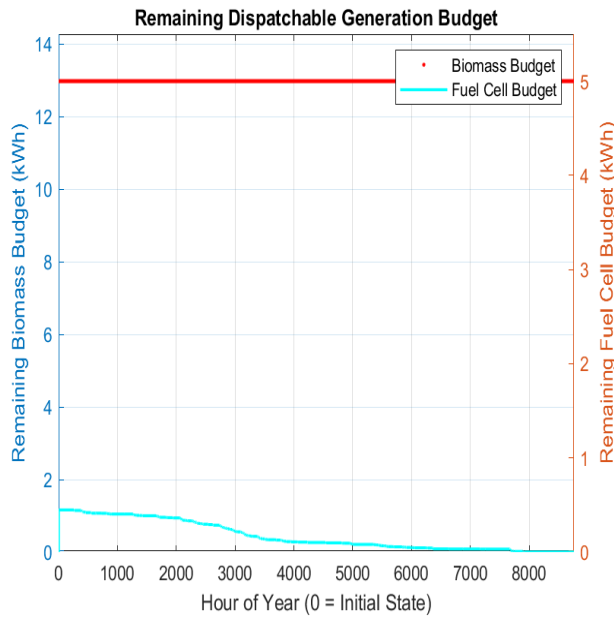


Figure 32. Remaining dispatchable generation budget for Onguati village throughout the year

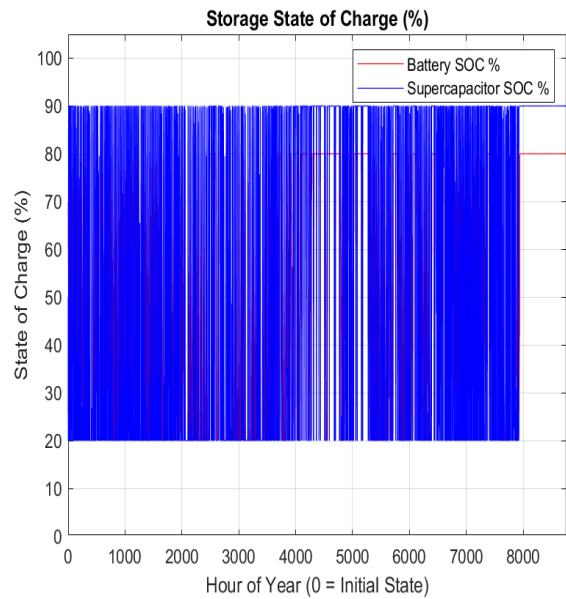


Figure 33. Battery and supercapacitor state-of-charge trends for Onguati village throughout the annual operation

Capacity Factors of Energy Sources

Error! Reference source not found. shows capacity factors (CFs) across energy sources. Solar CF is consistent at ~25% across all sites. Wind CF is below 15%, with Onguati achieving the highest wind contribution due to limited biomass. Biomass CF varies, Ombudiy a (~39%) and Oluundje (~27%), reflecting population size and resource availability. Fuel cell CF remains low (<8%), aligning with their backup role.

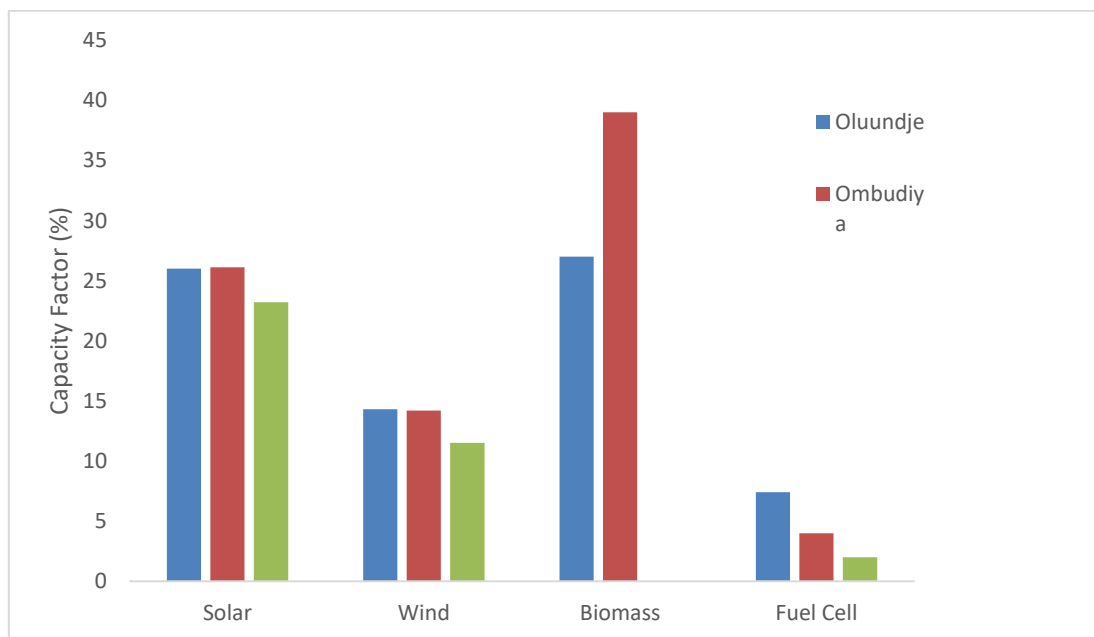


Figure 34. Capacity factors for the different energy sources for the different villages

Energy Composition of Energy Sources

Error! Reference source not found. to Figure 37 illustrates that RES vary from one rural area to another, stressing the need for an adaptable and optimal model that will ensure the sustainability of electricity supply despite the variations. Biomass dominates in Oluundje and Ombudiya (>45% share) villages. In Onguati, wind provides the largest share due to scarcity of Biomass resources. Solar plays a complementary role in all villages, while fuel cells contribute minimally, primarily for backup supply.

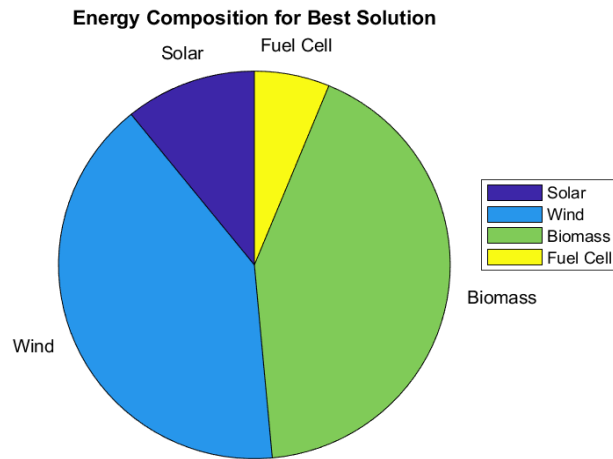


Figure 35. Oluundje village energy sources' composition

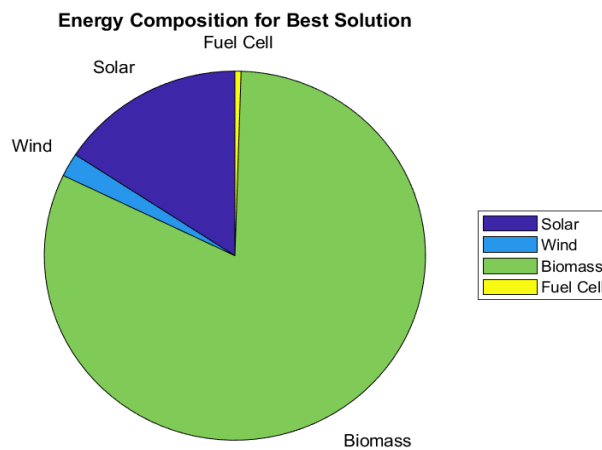


Figure 36. Ombudiya village energy sources' composition

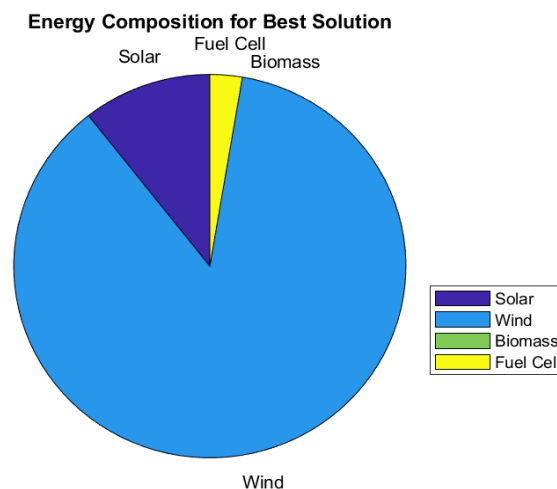


Figure 37. Onguati village energy sources' composition

Comparison with Existing Optimization Models

To demonstrate the superior performance of the proposed optimization model in achieving sustainability and adaptability to different geographical rural areas, the performance of the proposed NSGA-II optimization model was compared with existing models, as shown in **Table 4**. It was established that NSGA-II achieved high reliability at the lowest cost.

Table 4. Comparison of the developed model to models in literature

Model/Study	Location/Scope	LCOE(USD/kWh)	Reliability (%)	Key Notes
HOMER model [20]	Namibia	0.436	Not considered	No reliability factor evaluated
Grey Wolf Optimization		0.268	87.79	Optimized configuration for rural electrification
Harris Hawks Optimization	Namibia	0.276	82.85	Reliability slightly lower than GWO
HOMER model [37]		0.98	98.6	Highest reliability in [38] but very high cost
MS-Excel VBA SHS model [38]	Namibia	0.19	95	Designed for solar home systems
PSO model [21]	Namibia	0.12	96.3	Achieved high reliability and low cost
	Namibia (Oluundje)	0.0042	99.82	Lowest cost and highest reliability among all studies
NSGA-II model (this study)	Namibia (Ombudiya)	0.0023	79.82	Lowest cost overall but lowest reliability (trade-off observed)
	Namibia (Onguati)	0.0811	94.20	Balanced cost and reliability

CONCLUSION

This paper presents a comprehensive multi-objective optimization model for the optimal sizing and integration of HRES, tailored to rural electrification in Namibia. NSGA-II was implemented to minimize critical techno-economic and environmental objectives, including the *TLCC*, *LCOE*, *LPSP*, CO_2 emissions, and total wasted renewable energy. To refine the selection process among Pareto-optimal solutions, a weighted decision-making method was introduced, prioritizing cost and reliability, which are crucial factors for sustainable rural electrification.

The model was validated through detailed case studies in three Namibian villages: Oluundje, Ombudiya, and Onguati. Each case study incorporated site-specific load estimations, RERs assessments, and socio-economic considerations. It was revealed that while solar and wind are abundant, their intermittent nature reduces their standalone viability. The algorithm highlighted the importance of leveraging local bioenergy resources in combination with intermittent renewables and appropriately sized energy storage systems. The optimal configurations for the three villages, Oluundje, Ombudiya, and Onguati, in terms of *LCOE* were 0.0042 USD/kWh, 0.0023 USD/kWh and 0.0811 USD/kWh respectively, and all had reliabilities above 79.82%.

Overall, the proposed optimization framework provides a reliable, cost-effective, and scalable blueprint for rural electrification. Its application can inform policymakers, developers, and energy planners in Namibia and other developing regions with similar

socio-environmental contexts. Future work may focus on extending the model to include demand-side management, electrification growth projections, and community-level participation for enhanced sustainability and resilience. Furthermore, CO₂ emissions were kept as a separate objective to allow a clear assessment of environmental impacts, but future work could incorporate carbon pricing to integrate these effects into the economic objective and reduce problem dimensionality.

REFERENCES

1. K. Nyarko, J. Whale, and T. Urmee, Drivers and challenges of off-grid renewable energy-based projects in West Africa: A review, *Heliyon*, Vol. 9, No. 6, e16710, Jun. 2023, <https://doi.org/10.1016/J.HELIYON.2023.E16710>.
2. Q. Hassan, S. Algburi, A. Z. Sameen, H. M. Salman, and M. Jaszczur, A review of hybrid renewable energy systems: Solar and wind-powered solutions: Challenges, opportunities, and policy implications, *Results Eng.*, Vol. 20, 101621, Dec. 2023, <https://doi.org/10.1016/J.RINENG.2023.101621>.
3. R. Shaha, D. P. Kothari, and V. S. Chandrakar, Optimization of renewable energy sources for hybrid power generation, *Bienn. Int. Conf. Power Energy Syst. Towar. Sustain. Energy, PESTSE 2016*, 2016, <https://doi.org/10.1109/PESTSE.2016.7516527>.
4. A. Mohammad-Alikhani, A. Mahmoudi, and S. Kahourzade, Multi-objective optimization of system configuration and component capacity in AC mini-grid hybrid power system, *9th IEEE Int. Conf. Power Electron. Drives Energy Syst. PEDES 2020*, Dec. 2020, <https://doi.org/10.1109/PEDES49360.2020.9379526>.
5. B. Akbas, A. S. Kocaman, D. Nock, and P. A. Trotter, Rural electrification: An overview of optimization methods, *Renew. Sustain. Energy Rev.*, Vol. 156, 111935, Mar. 2022, <https://doi.org/10.1016/J.RSER.2021.111935>.
6. E. I. Come Zebra, H. J. van der Windt, G. Nhumaio, and A. P. C. Faaij, A review of hybrid renewable energy systems in mini-grids for off-grid electrification in developing countries, *Renew. Sustain. Energy Rev.*, Vol. 144, 111036, 2021, <https://doi.org/10.1016/J.RSER.2021.111036>.
7. H. Nabipour-Afrouzi, S. H. Wen Yii, J. Ahmad, and M. Tabassum, Comprehensive review on appropriate sizing and optimization technique of hybrid PV-wind system, *Asia-Pacific Power Energy Eng. Conf. APPEEC*, Vol. 2018, pp 364–369, 2018, <https://doi.org/10.1109/APPEEC.2018.8566269>.
8. R. F. Dad and S. Saleem, A Comparative Study of Various Optimization Techniques to Size a Hybrid Renewable Energy System, *2022 24th Int. Multitopic Conf. INMIC 2022*, 2022, <https://doi.org/10.1109/INMIC56986.2022.9972951>.
9. A. Maheri, MOHRES, a Software Tool for Analysis and Multiobjective Optimisation of Hybrid Renewable Energy Systems-An Overview of Capabilities, *Proc. 2021 6th Int. Symp. Environ. Energies Appl. EFEA 2021*, Mar. 2021, <https://doi.org/10.1109/EFEA49713.2021.9406221>.
10. S. Husain and N. A. Shrivastava, A Comparative Analysis of Multi-objective Optimization Algorithms for Stand-Alone Hybrid Renewable Energy System, *2nd Int. Conf. Innov. Mech. Ind. Appl. ICIMIA 2020 - Conf. Proc.*, pp 255–260, Mar. 2020, <https://doi.org/10.1109/ICIMIA48430.2020.9074903>.
11. A. Jain, S. Lalwani, and M. Lalwani, A Comparative Analysis of MOPSO, NSGA-II, SPEA2 and PESA2 for Multi-Objective Optimal Power Flow, *2nd Int. Conf. Energy, Power Environ. Towar. Smart Technol. ICEPE 2018*, 2018, <https://doi.org/10.1109/EPETSG.2018.8659054>.

12. A. Mohamad Izdin Hlal, V. K. Ramachandaramurthya, B. Sanjeevikumar Padmanaban, C. Hamid Reza Kaboli, A. Aref Pouryekt, and D. Tuan Ab Rashid Bin Tuan Abdullah, NSGA-II and MOPSO based optimization for sizing of hybrid PV / wind / battery energy storage system, *Int. J. Power Electron. Drive Syst.*, Vol. 10, No. 1, pp 463–478, Mar. 2019, <https://doi.org/10.11591/IJPEDS.V10.I1.PP463-478>.
13. X. Zhu, P. Gui, X. Zhang, Z. Han, and Y. Li, Multi-objective optimization of a hybrid energy system integrated with solar-wind-PEMFC and energy storage, *J. Energy Storage*, Vol. 72, p. 108562, Nov. 2023, <https://doi.org/10.1016/J.EST.2023.108562>.
14. P. Vijai and P. Bagavathi Sivakumar, A hybrid multi-objective optimization approach with NSGA-II for feature selection, *Decis. Anal. J.*, Vol. 14, p. 100550, Mar. 2025, <https://doi.org/10.1016/J.DAJOUR.2025.100550>.
15. D. P. Pinto-Roa, J. C. Mello-Román, J. L. V. Noguera, R. Quintana, F. Roa, and P. E. Gardel-Sotomayor, Multi-objective Evolutionary Algorithms based Operation Sequence Design for Image Segmentation, *CLEI Electron. J.*, Vol. 27, No. 4, pp 4:1-4:28, Sep. 2024, <https://doi.org/10.19153/CLEIEJ.27.4.4>.
16. G. Prinsloo, R. Dobson, and A. Mammoli, Smart Village Load Planning Simulations in Support of Digital Energy Management for Off-grid Rural Community Microgrids, *Curr. Altern. Energy*, Vol. 2, No. 1, pp 2–18, Nov. 2017, <https://doi.org/10.2174/2405463102666171122161858>.
17. M. Hasan et al., A state-of-the-art comparative review of load forecasting methods: Characteristics, perspectives, and applications, *Energy Convers. Manag. X*, Vol. 26, p. 100922, Apr. 2025, <https://doi.org/10.1016/J.ECMX.2025.100922>.
18. S. Kühnel et al., Holistic approach to develop electricity load profiles for rural off-grid communities in sub-Saharan Africa, *Proc. - ISES Sol. World Congr. 2021*, pp 348–361, 2021, <https://doi.org/10.18086/SWC.2021.20.02>.
19. J. Namaganda-Kiyimba, J. Mutale, and B. Azzopardi, Improving the Load Estimation Process in the Design of Rural Electrification Systems, *Energies 2021*, Vol. 14, Page 5505, Vol. 14, No. 17, p. 5505, Sep. 2021, <https://doi.org/10.3390/EN14175505>.
20. E. Hamatwi, C. N. Nyirenda, and I. E. Davidson, Optimisation of a hybrid PV-diesel system for rural application: The case of Oluundje village, Namibia, *Int. Sci. Technol. J. Namibia*, Vol. 9, pp 009–025, Jan. 2018, https://www.researchgate.net/publication/313477718_Optimisation_of_a_Hybrid_PV-Diesel_System_for_Rural_Application_The_Case_of_Oluundje_Village_Namibia, [Accessed: Sep. 01, 2025].
21. T. Wanjekeche and T. Ananias, Optimal and Economic Evaluation of a Stand-alone Microgrid for Electricity and Water Supply for Namibia’s Rural Village, *Am. J. Energy Eng. 2019*, Vol. 7, Page 64, Vol. 7, No. 3, pp 64–73, Nov. 2019, <https://doi.org/10.11648/J.AJEE.20190703.12>.
22. A. M. Patel and S. K. Singal, Renewable Energy Source based Hybrid Power Generation Scheme for Off-grid Rural Electrification, *2017 14th IEEE India Counc. Int. Conf. INDICON 2017*, Oct. 2018, <https://doi.org/10.1109/INDICON.2017.8487807>.
23. T. N. Rateele and L. Z. Thamae, An optimization approach for the economic dispatch incorporating renewable energy resources into Lesotho power sources portfolio, *Heliyon*, Vol. 9, No. 4, e14748, 2023, <https://doi.org/10.1016/J.HELİYON.2023.E14748>.
24. T. Baloyi, S. K. Kibaara, and S. Chowdhury, Economic feasibility analysis of wind and biomass-based electricity generation for rural South Africa, *IEEE PES PowerAfrica Conf. PowerAfrica 2016*, pp 306–310, 2016, <https://doi.org/10.1109/POWERAFRICA.2016.7556622>.
25. A. Jain, P. Das, S. Yamujala, R. Bhakar, and J. Mathur, Resource potential and variability assessment of solar and wind energy in India, *Energy*, Vol. 211, 118993, Nov. 2020, <https://doi.org/10.1016/J.ENERGY.2020.118993>.

26. M. Amaro Pinazo and J. L. Romeral Martinez, Intermittent power control in wind turbines integrated into a hybrid energy storage system based on a new state-of-charge management algorithm, *J. Energy Storage*, Vol. 54, 105223, Oct. 2022, <https://doi.org/10.1016/J.EST.2022.105223>.
27. C. Pang, J. Yu, and Y. Liu, Correlation analysis of factors affecting wind power based on machine learning and Shapley value, *IET Energy Syst. Integr.*, Vol. 3, No. 3, pp 227–237, 2021, <https://doi.org/10.1049/ESI2.12022>.
28. A. Askarzadeh and L. dos Santos Coelho, A novel framework for optimization of a grid independent hybrid renewable energy system: A case study of Iran, *Sol. Energy*, Vol. 112, pp 383–396, 2015, <https://doi.org/10.1016/J.SOLENER.2014.12.013>.
29. G. Jothiprakash, P. Balasubramaniam, S. Sundaram, and D. Ramesh, Catalytic Biomass Gasification for Syngas Production: Recent Progress in Tar Reduction and Future Perspectives, *Biomass 2025*, Vol. 5, Page 37, Vol. 5, No. 3, p. 37, Jun. 2025, <https://doi.org/10.3390/BIOMASS5030037>.
30. P. Brahamne, A. P. M. P.. S. Chawla, and D. H. K. Verma, Optimal Sizing of Hybrid Renewable Energy System using Manta Ray Foraging Technique, *Int. J. Emerg. Sci. Eng.*, Vol. 11, No. 3, pp 8–16, 2023, <https://doi.org/10.35940/IJESE.C2545.0211323>.
31. F. H. Malik, G. A. Hussain, Y. M. S. Alsmadi, Z. M. Haider, W. Mansoor, and M. Lehtonen, Integrating Energy Storage Technologies with Renewable Energy Sources: A Pathway Toward Sustainable Power Grids, *Sustain. 2025*, Vol. 17, Page 4097, Vol. 17, No. 9, p. 4097, May 2025, <https://doi.org/10.3390/SU17094097>.
32. A. Z. AL Shaqsi, K. Sopian, and A. Al-Hinai, Review of energy storage services, applications, limitations, and benefits, *Energy Reports*, Vol. 6, pp 288–306, Dec. 2020, <https://doi.org/10.1016/J.EGYR.2020.07.028>.
33. R. R. Thakkar, Electrical Equivalent Circuit Models of Lithium-ion Battery, *Manag. Appl. Energy Storage Devices*, 2021, <https://doi.org/10.5772/INTECHOPEN.99851>.
34. F. Naseri, S. Karimi, E. Farjah, and E. Schaltz, Supercapacitor management system: A comprehensive review of modeling, estimation, balancing, and protection techniques, *Renew. Sustain. Energy Rev.*, Vol. 155, 111913, 2022, <https://doi.org/10.1016/J.RSER.2021.111913>.
35. A. Satyanarayana and I. E. S. Naidu, Modeling and Analysis of Fuel Cell Power Generation System Using Proportional Integral Speed Controller, *Adv. Sci. Technol. Res. J.*, Vol. 18, No. 2, pp 187–195, 2024, <https://doi.org/10.12913/22998624/184340>.
36. C. B. Amougou, D. Tsuanyo, D. Fioriti, J. Kenfack, A. Aziz, and P. Elé Abiama, LCOE-Based Optimization for the Design of Small Run-of-River Hydropower Plants, *Energies*, Vol. 15, No. 20, Oct. 2022, <https://doi.org/10.3390/EN15207507>.
37. R. Ouederni and I. E. Davidson, Co-Optimized Design of Islanded Hybrid Microgrids Using Synergistic AI Techniques: A Case Study for Remote Electrification, *Energies*, Vol. 18, No. 13, 3456, 2025, <https://doi.org/10.3390/EN18133456>.
38. P. E. Campana et al., An open-source optimization tool for solar home systems: A case study in Namibia, *Energy Convers. Manag.*, Vol. 130, pp 106–118, Dec. 2016, <https://doi.org/10.1016/J.ENCONMAN.2016.10.003>.



Paper submitted: 02.09.2025
Paper revised: 04.01.2026
Paper accepted: 13.01.2026